Ab initio study of the C2O+ cation

Laurent Jutier, Céline Léonard

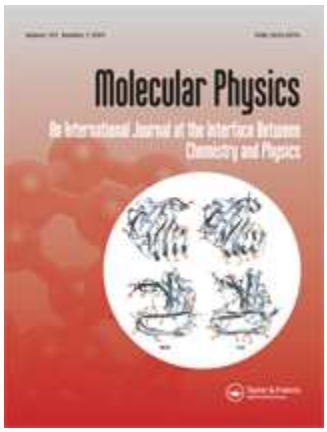

Ab initio study of the C2O+ cation

Journal:	*Molecular Physics*
Manuscript ID:	TMPH-2006-0100
Manuscript Type:	Full Paper
Date Submitted by the Author:	27-Nov-2006
Complete List of Authors:	Jutier, Laurent; Universite de Marne la Vallee leonard, celine; Universite de Marne la Vallee
Keywords:	CCO, ab initio spectroscopy, electronic potentials, rovibrational levels, spin-orbit coupling

Ab initio study of the C_2O^+ cation

L. Jutier and C. Léonard

Université de Marne la Vallée, Laboratoire de Chimie Théorique, EA 2180, 5 bd Descartes, Champs-sur-Marne - 77454 Marne la Vallée Cedex 2 - France

Abstract

The first electronic states of C_2O^+ correlating to the first asymptotes of dissociation are presented. From accurate MRCI+Q / cc-pV5Z calculations, it is shown that the electronic ground state is the $X^2\Pi$ state and the first excited state the $a^4\Sigma^-$ state lying very close to the $X^2\Pi$ state, $E^{eq}(^4\Sigma^-) - E^{eq}(^2\Pi) = 2388$ cm^{-1}. For both states, the 3-dimensional PEFs are determined for displaced geometries in the range $-0.35 \lesssim \Delta R_{CC} \lesssim +0.6$ bohr, $-0.2 \lesssim \Delta R_{CO} \lesssim +0.3$ bohr about the equilibrium bond lenghts and $150° \leq \hat{CCO} \leq 180°$. The rovibronic levels up to 2200 cm^{-1} and $J = P = 7/2$ are obtained for $X^2\Pi$ and the rovibrational levels of $^4\Sigma^-$ up to 5000 cm^{-1} and $K = 4$. The spin-orbit coupling between both states is investigated.

November 27, 2006

Corresponding author :
Dr. Céline LEONARD
Université Marne la Vallée
Laboratoire de Chimie Théorique - Bâtiment Lavoisier
5 boulevard Descartes - Champs sur Marne
77454 MARNE LA VALLEE CEDEX 2
FRANCE
Tel : +33.1.60.95.73.18
Fax : +33.1.60.95.73.20
Email : celine.leonard@univ-mlv.fr

1 Introduction

The molecular cation C_2O^+ plays an important role in the chain reactions which take place in the interstellar clouds involving the monoatomic fragments C, C^+, O, O^+ and diatomic C_2, C_2^+, CO, CO^+, O_2, O_2^+ from which C_2O^+ can be formed. In particular, C_2O^+ can be produced by the ion-neutral reaction of CO [1]. Furthermore, this cation is a link towards molecular cations of C_nO^+ type, with $n > 2$. Some of the occuring mechanisms have already been identified twenty five years ago, using mass spectroscopy, by Schildcrout and Franklin [2].

In 1982, Haese and Woods [3] performed *ab initio* calculations on the electronic states of C_2O^+, and established that the most stable isomer is the linear $[C\text{-}C\text{-}O]^+$. They presented a $^2\Pi$ for the ground state, which is in agreement with the more recent works performed by Maclagan and Sudkeaw in 1993 [4], who also calculated the harmonic vibrational frequencies of the $^2\Pi$ state.

In 1995, Cao and Tian [5] studied theoretically the reactions $\{C_2^+ + CO\}$ and $\{C_2^+ + O\}$. They found that the reaction product is mostly C_2O^+ in the $^4\Sigma^-$ state in both cases and they computed harmonic frequencies for this state. But there is still an uncertainty about the nature of the ground electronic state.

The objective of the present *ab initio* study is to obtain an accurate relative position of the $^2\Pi$ and the $^4\Sigma^-$ energies. In a first part, all the electronic states associated to the first dissociation asymptotes are studied, showing that the minima of the first $^2\Pi$ and $^4\Sigma^-$ states are close to each other and are much lower than the other states. Then, the second part of this work is devoted to accurate electronic calculations of these both states in order to confirm the nature of the ground state. Moreover, using new *ab initio* potential energy functions, the rovibronic energies corresponding to these lowest electronic states are computed variationaly. The study is completed by an investigation of the spin-orbit coupling between the $^2\Pi$ and $^4\Sigma^-$ states.

2 Study of the first electronic states

2.1 Asymptotes of dissociation

All the molecular electronic states belonging to the first three asymptotes of dissociation are studied. Relative energies of these asymptotes are already known from Moore [6] for atomic fragments, Huber and Herzberg [7] for CO and CO^+ and Wang, Zhu and Yang [8] for C_2^+. The corresponding states for linear geometries are reported in Table 1. The dissociation along CO shows a high density of states: 6 doublets, 6 quartets and 2 sextets states are distributed in the two first asymptotes separated by less than 8000 cm^{-1}. These asymptotes are associated to the first electronic states of C_2^+ combined with O in its electronic ground state ^3P_g. For

this molecule, the ambiguity concerning the nature of the electronic ground state was raised very recently by Wang *et al.* [8]. They found that the electronic ground state is $X^4\Sigma_g^-$ with an equilibrium bond length of 2.672 bohr and the first excited electronic state is $a^2\Pi_u$ with R_{CC}^{eq} at 2.497 bohr. The dissociation along CC is by far less complicated. The first asymptote is due to the combination of C^+ and CO in their respective electronic ground states ^2P_u and $X^1\Sigma^+$ with $R_{CO}^{eq} = 2.132$ bohr [7]. The second and the third ones combine CO^+ in $X^2\Sigma^+$ with $R_{CO}^{eq} = 2.107$ bohr [7] with C in ^3P_g and ^1D_g. The density of states is smaller in that case with only 7 doublets and 2 quartets.

****

Table 1 near here

****

2.2 Linear cuts

Using the MOLPRO software [9], the energies of the molecular electronic states given in Table 1 are obtained at the Multi-Configuration Self Consistent Field (MCSCF) level [10, 11] with the correlation consistent polarized Valence Triple Zeta (cc-pVTZ) basis set [12] leading to a total of 90 contracted s, p, d and f gaussian functions. The active space comprised all the valence molecular orbitals (OMs) and all the states associated to a given spin multiplicity are averaged alltogether with one set of optimised OMs. Figures 1 and 2 present the linear cuts of the electronic states of Table 1 dissociating along CC and CO respectively. The computations were done in the C_{2v} symmetry group and the non-dissociating part of the molecule was not relaxed. In the first case, R_{CO} is fixed arbitrarily at 2.15 bohr and in the second one R_{CC} at 2.60 bohr, these values being close to the isolated diatomic bond lengths. The density of states in Figure 2 is as large as expected from Table 1 and the avoided-crossings occur for large values of R_{CO}. In Figure 1 the number of states is smaller but the complexity comes from the mixing between the states occuring in the equilibrium region of the lowest states.

****

Figures 1 and 2 near here

****

Both figures show that the lowest electronic states are a $^4\Sigma^-$ and a $^2\Pi$ states. The $^4\Sigma^-$ state is correlated to the $\{ CO^+[^2\Sigma^+]+C[^3P_g]\}$ and the $\{C_2^+[^2\Pi_u]+O[^3P_g]\}$ asymptotes and the $^2\Pi$ state to the $\{CO[^1\Sigma^+]+C^+[^2P_u]\}$ and the $\{C_2^+[^4\Sigma_g^-]+O[^3P_g]\}$ asymptotes. At this level of computation, the electronic ground state of C_2O^+ is the $^4\Sigma^-$ state. The different behaviour of

both states in the CC dissociation for large R_{CC} is certainly linked to the interactions between the different fragments. In the case of the $^4\Sigma^-$ state, the interaction between $CO^+(X^2\Sigma^+)$ and C corresponds to an ion-quadrupole interaction which behaves like $\sim -1/R_{CC}^3$. Whereas for the $^2\Pi$ state, CO + C^+ corresponds to a ion-polarisability interaction which behaves like $\sim -1/R_{CC}^4$ since CO is almost apolar [13].

2.3 Linear equilibrium geometries

The linear equilibrium geometries of the first doublet and quartet states have been optimised and are reported in Table 2 with the corresponding energies and the predominant electronic configuration. The values confirm that the lowest $^4\Sigma^-$ state seems to be the ground electronic state separated by only 0.011645 a.u., i.e. 0.32 eV from the lowest $^2\Pi$ state. This value is relatively close to the separation of 0.93 eV between the $X^4\Sigma_g^-$ and the $^2\Pi_u$ states in C_2^+. Table 2 and Figures 1 and 2 show also that the $^2\Pi$ state has a floppier minimum along R_{CC} than the $^4\Sigma^-$ state associated with a different value of R_{CC}^{eq} (in agreement with the equilibrium bond lengths of the correlating electronic states of the C_2^+ fragment [8]), whereas both states present similar values of R_{CO}^{eq} and similar steepness around the minimum along R_{CO}. These equilibrium geometries are in agreement with previous *ab initio* values [4] and [5]. The cut along the CC dissociation presents a crossing of these two states for a value of R_{CC} intermediate between the equilibrium positions of $^4\Sigma^-$ and $^2\Pi$. This behaviour seems typical of the CC bond length since it has been already found in the diatomic C_2^+ by Wang *et al.* [8] and in the larger system $[HCCO]^+$ by Papakondylis and Mavridis [14].

For each spin multiplicity, there is a difference between the geometry of the lowest state and the geometries of the excited states which have similar equilibrium geometries.

****

Table 2 near here

****

2.4 Bent cuts

The variation of the potential of the lowest doublet and quartet electronic states with the bending angle was investigated. The doublet and the quartet states have been computed independently using the C_s symmetry for all the points. The variation of the energy of the doublet states with the bending angle is shown in Figure 3 and in Figure 4 for the quartet states. The bond lengths were fixed at the equilibrium geometry of the lowest $^2\Pi$ state and of the lowest $^4\Sigma^-$ state for the doublet and the quartet states respectively. The two Renner-Teller

components (A' and A'') of the Π and Δ states split up when $\theta = C\hat{C}O \leq 180°$. All the states present a floppy minimum at $\theta = 180°$, except the $^4\Pi$ state. Avoided crossings occur in both $^2A'$ and $^2A''$ symmetries for $\theta < 140°$ provoking deep minima particularly for the excited $^2A'$ states. An avoided crossing for θ at about 95° induces a second minimum in the component $^2A'$ of the lowest $^2\Pi$ state for $\theta \approx 60°$. For the quartet states, the avoided crossings appear for $\theta < 160°$. In general, the variation of the energy with the bending coordinate is larger in the quartet states than in the doublet states.

****

Figures 3 and 4 near here

****

3 Specific study of the lowest $^2\Pi$ and $^4\Sigma^-$ electronic states

3.1 Determination of the electronic ground state

From the results of the previous section, the inclusion of more electronic correlation in the electronic treatment is necessary in order to confirm if the $^4\Sigma^-$ state is the electronic ground state of C_2O^+. After a MCSCF step producing a reference wavefunction, the Internally Contracted Multi-Reference Configuration Interaction (MRCI) method [15, 16] including the multireference Davidson correction [17] (MRCI+Q) is applied to the lowest $^4\Sigma^-$ state and to each electronic component of the lowest $^2\Pi$ state separately. For the $^2\Pi$ state, the two Renner-Teller components are averaged together at the MCSCF level. The equilibrium geometry of these states was obtained using different basis sets. Table 3 shows that the equilibrium bond lengths and energies of both states decrease with the size of the basis set. But Table 3 shows also the variation of the energy difference $\Delta E = E^{eq}(^4\Sigma^-) - E^{eq}(^2\Pi)$ with the basis. This difference is positive for all the basis set and seems also to converge at 2388 cm^{-1} for the cc-pV5Z basis set [12] (giving a total of 273 contracted s, p, d, f, g and h gaussian functions). This basis set will be used in order to determine the potential energy functions (PEFs) of both states in the following part of the study.

****

Table 3 near here

****

Contrary to the global study of the large set of electronic states with averaged molecular orbitals, at the MRCI+Q level, the electronic ground state is always the $^2\Pi$ state, showing that

the static correlation must be included in order to place correctly the $^2\Pi$ state with respect to the $^4\Sigma^-$. We checked that this relative order is the same at the MRCI level.

3.2 Determination of the PEFs

The MRCI+Q / cc-pV5Z electronic energy was computed for 33 geometries around the respective equilibrium geometry for both the $a^4\Sigma^-$ and the $X^2\Pi$ electronic states. All the points (24 linear and 9 non-linear) were performed in the C_s symmetry group.

For the doublet state, the geometries spread over a range such as: $2.56 \leq R_{CC} \leq 3.50$ bohr, $1.91 \leq R_{CO} \leq 2.41$ bohr and $150° \leq \theta \leq 180°$. For the quartet state: $2.17 \leq R_{CC} \leq 3.10$ bohr, $1.93 \leq R_{CO} \leq 2.43$ bohr and $150° \leq \theta \leq 180°$.

These points were fitted by a polynomial expansion up to the sixth order of R_{CC} and to the fourth order of R_{CO} and θ:

$$V(R_{CC}\,,\,R_{CO}\,,\,\theta) = \sum_{ijk} C_{ijk}(R_{CC} - R_{CC}^{eq})^i(R_{CO} - R_{CO}^{eq})^j(\theta - \pi)^k \qquad (1)$$

with $0 \leq i \leq 6$, $0 \leq j,k \leq 4$, $0 \leq i+j+k \leq 4$ and k must always be even in order to respect the symmetry of the bending mode. The reference is chosen as the equilibrium geometry (defined as the geometry for which the first derivatives of the PEF are zero) of the given state. The 24 expansion coefficients, optimised in a least square fitting with a Root Mean Square (RMS) of 0.4 cm^{-1}, are given in Table 4 with the reference geometries. The coefficient C_{002}, associated to the square of the bending displacement, of the two linear-linear Renner-Teller components of the $X^2\Pi$ state confirms that the lower component is $^2A''$ as shown in Figure 3 for large values of θ.

The norm of the equilibrium dipole moment, the reference being the center of mass of the molecule, is given for both states in Table 4 as additional data.

****

Table 4 and Figure 5 near here

****

Figure 5 shows the 2D crossing between the $X^2\Pi$ and $a^4\Sigma^-$ states for the linear geometries. The crossing surface is almost independent of R_{CC} and the minimum is at $R_{CC} = 2.574$ bohr and $R_{CO} = 2.140$ bohr, 2434 cm^{-1} above the $X^2\Pi$ minimum and very close to the equilibrium of the $a^4\Sigma^-$ state (cf Table 4).

The harmonic and anharmonic constants are obtained from the PEFs derivatives at the minima [18, 19], and are given in Table 5 with the equilibrium rotational constants for both

electronic states. The harmonic wavenumbers predict a Fermi coupling in the $X^2\Pi$ state between the modes 1 and 2. This Renner-Teller state presents also strong anharmonic constants when the bending is involved in the A' component. This could be linked to the avoided crossing occuring in this component for $\theta \approx 95°$ (cf. Figure 3). Moreover, the values of ω_1 and ω_2 are approximatively twice in the quartet state than in the doublet state, whereas ω_3 are identical in both states.

The definitions of the stretching normal modes are given in Table 6 showing that, for both electronic states, Q_3 corresponds almost completely to the stretching of the CO bond whereas Q_1 is mostly associated to the CC stretch with a small mixing with the CO stretch. The mixing between the two bond stretches is slightly stronger for the $a^4\Sigma^-$ state than for the $X^2\Pi$ state in relation with the fact that the harmonic wavenumbers ω_1 and ω_3 are closer in the quartet state. This mixing is also caracterised by a large value of x_{13} in the $a^4\Sigma^-$ state.

****

Tables 5 and 6 near here

****

3.3 Spin-orbit coupling

The spin-orbit interaction was calculated between the $X^2\Pi$ and $a^4\Sigma^-$ states and between the 4 spin-electronic components of the $X^2\Pi$ state. The spin-orbit coupling can be treated perturbatively and the coupling terms are the matrix elements of the non-relativistic part of the Breit-Pauli operator $\hat{H}_{SO}^{BP}$ [20, 21] on the basis of the spin-electronic wavefunctions. The wavefunctions were obtained with the MCSCF method and the uncontracted s, p and d functions of the cc-pV5Z basis set. The z axis corresponds to the linear molecular axis and x-axis bisects the bond angle θ. For the $X^2\Pi$ state, the couplings between the different components can be determined from:

$$LS_z = \langle A'\phi_{S=1/2}^{\sigma=1/2}|\hat{H}_{SO}^{BP}|A''\phi_{S=1/2}^{\sigma=1/2}\rangle = iA \qquad (2)$$

A equals -22.52 cm^{-1} at the equilibrium geometry leading to a spin-orbit constant $A_{SO} = -2A = 45.05$ cm^{-1} (cf. ref [21]). This positive value is in agreement with a normal multiplet splitting and is comparable with the spin-orbit splitting of 43.5 cm^{-1} between the $^3P_{g0}$ and $^3P_{g2}$ states of the carbon atom [6]. The LS_z integral has been calculated for all the geometries of the grid used for the $X^2\Pi$ state and the corresponding A values have been fitted using the polynomial expansion of equation 1 with the same restrictions on i, j and k. The corresponding coefficients are given in Table 7. The fitted function has been obtained with a RMS of 10^{-8} a.u. The variations of A with the geometry are shown in Figure 6.

****

Figure 6 near here

****

The coupling terms between the $X^2\Pi$ and $a^4\Sigma^-$ states are given by:

$$LS_x^1 = \langle A'\phi_{S=1/2}^{\sigma=1/2}|\hat{H}_{SO}^{BP}|A''\phi_{S=3/2}^{\sigma=1/2}\rangle \quad (3)$$

$$LS_y^1 = \langle A''\phi_{S=1/2}^{\sigma=1/2}|\hat{H}_{SO}^{BP}|A''\phi_{S=3/2}^{\sigma=3/2}\rangle \quad (4)$$

with $LS_x^1 = iLS_y^1$.

$$LS_x^2 = \langle A'\phi_{S=1/2}^{\sigma=1/2}|\hat{H}_{SO}^{BP}|A''\phi_{S=3/2}^{\sigma=-1/2}\rangle = \frac{-LS_x^1}{\sqrt{3}} \quad (5)$$

$$LS_y^2 = \langle A''\phi_{S=1/2}^{\sigma=1/2}|\hat{H}_{SO}^{BP}|A''\phi_{S=3/2}^{\sigma=-1/2}\rangle = \frac{LS_y^1}{\sqrt{3}} \quad (6)$$

with also $LS_x^2 = iLS_y^2$.

As an example, a zoom of the region of the crossing between the $X^2\Pi$ and $a^4\Sigma^-$ states including the spin-orbit coupling is shown in Figure 7 for R_{CO} fixed at 2.123 bohr $\approx R_{CO}^{eq}(X^2\Pi)$. The first avoided crossing occurs at $R_{cc} = 2.6402$ bohr with a splitting of 5.77 cm^{-1} between the $\Omega = 1/2$ components and the second avoided crossing at $R_{cc} = 2.6424$ bohr, the $\Omega = 3/2$ components being separated by 9.82 cm^{-1}. $|LS_y^1| = 3.47$ cm^{-1} for both crossings.

In conclusion, the spin-orbit coupling between the two electronic states is small and we checked that this coupling is almost not geometry dependent.

****

Figure 7 near here

****

3.4 Rovibronic levels

For a linear triatomic molecule, the vibrational angular momentum along the molecular axis is associated with the quantum number l where $l = v_2, v_2 - 2, ..., 1$ or 0, with v_2 the bending quantum number. If the electronic orbital angular momentum has a nonzero projection along the molecular axis z caracterized by the quantum number Λ, the Renner-Teller coupling between the electronic orbital and vibrational angular momenta forms a new quantum number, $K = |\Lambda \pm l|$. Including coupling of the projection of the spin angular momentum on the molecular axis, the projected angular momentum quantum number is now $P = |K \pm \sigma|$ and the final rovibronic levels are associated with terms:

$$^{(2S+1)}\{K\}_P \quad (7)$$

where $2S+1$ is the spin-multiplicity and $\{K\}$ is the notation for the different values of K: $K = 0$, 1, 2, 3 gives Σ, Π, Δ, Φ vibronic levels.

Using the code RVIB3 [22], the rovibronic levels of the $X^2\Pi$ state on one hand and the rovibrational levels of the $a^4\Sigma^-$ state on the other hand have been determined up to 2200 cm^{-1} and 5000 cm^{-1} respectively using the PEFs presented in Table 4. These two sets were treated independently.

For the doublet state, the internal spin-orbit interaction is included via the geometry dependant analytical representation of A (see Table 7) [21] and the rovibronic levels have been obtained for $J = P = 1/2$, $3/2$, $5/2$ and $7/2$, where J is the quantum number associated with the projection of the total angular momentum on the molecular axis. For the quartet state, the internal spin-vibrational coupling is not taken into account at the present time in the code RVIB3 and the rovibrational levels have been obtained for $J = K = 0$, 1, 2, 3 and 4.

For both states, the contraction scheme involves 25 harmonic oscillator eigenfunctions for each stretching mode and 41 Legendre polynomials for the bending mode as basis functions. The primitive set of integration points comprised 46 and 52 points for the stretching and the bending modes respectively. The resulting energies are given in Tables 8 and 9. The energy reference is the zero rovibrational energy of the corresponding electronic state. The density of levels is high for the $X^2\Pi$ state due to the spin-orbit and the Renner-Teller couplings, and the assignment of the levels above 2200 cm^{-1} becomes hazardous. The level noted * are tentatively assigned. Such levels are more numerous among the κ levels (associated with the A' component) than among the μ levels (associated with the A'' component) ; this results from the Fermi coupling and the strong anharmonicity for the levels associated to the A' component as predicted above. The vibrational levels of the quartet state are more separated in energy and they have been assigned up to 5000 cm^{-1}. Several levels are only tentatively labeled due to the Fermi coupling eventhough the harmonic wavenumbers do not emphasize this behaviour in the quartet state .

Since the minimum of the crossing surface ($R_{CO}, R_{CC}, \theta = 180°$) of both states occurs at 2434 cm^{-1} above the $X^2\Pi$ minimum, the presented levels of the doublet state should not be perturbated by the presence of the quartet state. Moreover, the rovibrational levels of the $a^4\Sigma^-$ state have been computed assuming that the $X^2\Pi$ and $a^4\Sigma^-$ states do not interfer by spin-orbit coupling. This assumption is confirmed by the following development. The spin-orbit coupling between vibrational levels v and v' corresponding to different spin-electronic states se and $s'e'$ can be seen, in the Born-Oppenheimer approximation, as the quantity:

$$\begin{aligned} SO_{vv'} &= \langle \Psi^{se}\Psi^{e}_{v}|\hat{H}_{SO}|\Psi^{s'e'}\Psi^{e'}_{v'}\rangle \\ &= \langle \Psi^{e}_{v}|\Psi^{e'}_{v'}\rangle\langle \Psi^{se}|\hat{H}_{SO}|\Psi^{s'e'}\rangle \end{aligned} \quad (8)$$

The first integral is the Franck-Condon factor. This factor is assumed to be rather large (but

never larger than 1) for the energy levels of the $a^4\Sigma^-$ state situated below 5000 cm^{-1} from the zero rovibrational energy due to the fact that the $X^2\Pi$ and $a^4\Sigma^-$ states intersect close to the equilibrium of the $a^4\Sigma^-$ state (cf. Figure 5). However, the second integral corresponds to quantities computed in equations 3 to 5 and is associated with small values (≈ 3.5 cm^{-1}). Moreover, the zero vibrational energy of the quartet state lies 2864 cm^{-1} above the zero vibrational energy of the doublet state, reaching a high density of vibronic levels region in the doublet state. It is very difficult to predict the accurate position of the levels in such a situation. Consequently the resonances between the $X^2\Pi$ and the $a^4\Sigma^-$ states rovibrational levels have not been investigated.

****

Tables 8 and 9 near here

****

3.5 Electronic transitions

In order to predict the possible transitions in UV absorption spectroscopy, the vertical transition moments and energies were computed at the equilibrium geometries of the $X^2\Pi$ and $^4\Sigma^-$ states. The results are presented in Table 10. The first transitions start from the $X^2\Pi$ state and reach the first $^2\Delta$, $^2\Sigma^+$ and $^2\Sigma^-$ electronic states. These transitions correspond to relatively large transition dipole moments. They should be observed between 450 and 300 nm. They should be caracterized by long progressions involving the stretching mode which is associated to the variation of CC bond length, i.e. ν_1 due to the strong difference of the CC equilibrium bond lengths between the $X^2\Pi$ and the excited doublet states (cf. Table 2). The first transition associated with quartet states involves the $a^4\Sigma^-$ and the first $^4\Pi$ electronic states and should be mesured at 232 nm, but the corresponding transition dipole moment is small (≈ 0.04 D).

****

Table 10 near here

****

In conclusion, at room temperature, $\frac{3}{2}kT = 308$ cm^{-1} if $T = 295$ K, the absorption spectra should only show transitions from the $X^2\Pi$ state since the $a^4\Sigma^-$ state is 2388 cm^{-1} above and the spin-orbit coupling is too small to couple these states efficiently.

4 Conclusion

This study has given a general view about the spectroscopy of the C_2O^+ cation where an ambiguity remained about the nature of the electronic ground state. The excited electronic states have been investigated showing that the lowest states are $X^2\Pi$ and $a^4\Sigma^-$. High level of configuration interaction calculations have allowed to guaranty that the electronic ground state is the Renner-Teller $^2\Pi$ state and that the first excited state is the $^4\Sigma^-$ state with an equilibrium transition energy, T_e, of 2388 cm^{-1}. In order to complete the study, the rovibrational levels of both states have been computed. It has been shown also that the spin-orbit coupling between these electronic states can be neglected. The knowledge of the electronic ground state has allowed to determine the vertical electronic transitions. These predictions will be useful for further experimental investigations of the spectroscopy of this cation.

Note : the *ab initio* points are available upon request.

5 Acknowledgments

The authors would like to thank P. Rosmus, G. Chambaud and F. Le Quéré for stimulating discussions.

References

[1] W. Lu, P. Tosi, and D. Bassi *J. Chem. Phys.*, vol. 111, p. 8852, 1999.

[2] S. M. Schildcrout and J. L. Franklin *J. Am. Chem. Soc.*, vol. 92, pp. 251 – 253, 1969.

[3] N. N. Haese and R. C. Woods *Chem. Phys. Lett.*, vol. 92, no. 3, pp. 190 – 192, 1982.

[4] R. G. A. R. Maclagan and P. Sudkeaw *J. Chem. Soc. : Faraday Trans.*, vol. 89, no. 18, pp. 3325 – 3329, 1993.

[5] Z. Cao and A. Tian *J. Mol. Struct. (Theochem)*, vol. 334, pp. 45 – 50, 1995.

[6] C. E. Moore, *Atomic Energy Levels, Vol. I; Circular of the National Bureau of Standards 467*. U.S. Government Printing Office, Washington, DC, 1949.

[7] K. P. Huber and G. Herzberg, *Constants of Diatomic Molecules*. D. Von Nostrand, Reinhold, 1979.

[8] R. Wang, Z. H. Zhu, and C. L. Yang *J. Mol. Struct. (Theochem)*, vol. 571, pp. 133 – 138, 2001.

[9] MOLPRO, a package of ab initio programs designed by H.-J. Werner and P.J. Knowles *et al.*, version 2002.6, www.molpro.net.

[10] H.-J. Werner and P. J. Knowles *J. Chem. Phys.*, vol. 82, p. 5053, 1985.

[11] P. J. Knowles and H.-J. Werner *Chem. Phys. Lett.*, vol. 115, p. 259, 1985.

[12] J. T. H. Dunning *J. Chem. Phys.*, vol. 90, p. 1007, 1989.

[13] M. A. Buldakov and V. N. Cherepanov *J. Phys. B*, vol. 37, pp. 3973 – 3986, 2004.

[14] A. Papakondylis and A. Mavridis *J. Phys. Chem. A*, vol. 109, pp. 6549 – 6554, 2005.

[15] H.-J. Werner and P. J. Knowles *J. Chem. Phys.*, vol. 89, p. 5803, 1988.

[16] P. J. Knowles and H.-J. Werner *Chem. Phys. Lett.*, vol. 145, p. 514, 1988.

[17] S. R. Langhoff and E. R. Davidson *Int. J. Quantum. Chem.*, vol. 8, p. 61, 1974.

[18] J. Senekowitch Master's thesis, University of Frankfurt, 1998.

[19] I. M. Mills, *Molecular Spectroscopy, Modern Research*. K. N. Rao, Academic Press, 1972.

[20] A. Berning, M. Schweizer, H.-J. Werner, P. Knowles, and P. Palmieri *Mol. Phys.*, vol. 21, p. 1823, 2000.

[21] C. Léonard, G. Chambaud, and S. Carter *Chem. Phys. Lett.*, vol. 398, pp. 123–129, 2004.

[22] S. Carter, N. C. Handy, C. Puzzarini, R. Tarroni, and P. Palmieri *Mol. Phys.*, vol. 98, p. 1697, 2000.

Figure captions:

Figure 1: linear dissociation of CCO^+ along R_{CC} (bohr) towards the first three asymptotes with MCSCF/cc-pVTZ computations.

Figure 2: linear dissociation of CCO^+ along R_{CO} (bohr) towards the first three asymptotes with MCSCF/cc-pVTZ computations.

Figure 3: variation of the energy of the first doublet electronic states with the bending coordinate from MCSCF/cc-pVTZ computations.

Figure 4: variation of the energy of the first quartet electronic states with the bending coordinate from MCSCF/cc-pVTZ computations.

Figure 5: 2D contour plots of the MRCI+Q / cc-pV5Z PEFs for the $X^2\Pi$ and $a^4\Sigma^-$ states for linear geometries. The full lines describe the $a^4\Sigma^-$ state and the dashed lines the $X^2\Pi$ state. The origin of energy is the minimum of the $X^2\Pi$ state, and the step among curves is 1000 cm^{-1}.

Figure 6: 1D cuts (a, b, c) of the variation of the spin-orbit coupling term A (see eq. 2) of the $X^2\Pi$ electronic state with R_{CC}, R_{CO} and θ. The other coordinates are respectively fixed to their equilibrium values: $R_{CC} = 2.8944$ bohr, $R_{CO} = 2.1235$ bohr and $\theta = 180°$.

Figure 7: Crossings between the $X^2\Pi$ and $a^4\Sigma^-$ electronic states including the spin-orbit coupling. The $\Omega = 1/2$ components are in full-lines and the $\Omega = 3/2$ components are in dashed lines where $\Omega = |\Lambda + \sigma|$ (Λ and σ are the quantum numbers associated with the projection along z of the total electronic orbital and spin angular momenta respectively).

Table 1: First asymptotes of dissociation in both cases : $\{CO + C\}^+$ or $\{C_2 + O\}^+$, and resulting molecular states. The energy reference is taken at the lowest energetic asymptote : $\{CO[^1\Sigma^+]+C^+[^2P_u]\}$. The fragment energies are taken from ref. [6], [7] and [8].

$R_{CC} \rightarrow \infty$:

Energy (cm^{-1})	Fragments		States for the linear molecule $[CCO]^+$
32345	$CO^+[^2\Sigma^+]$	$C[^1D_g]$	$^2\Sigma^+$, $^2\Pi$, $^2\Delta$
22151	$CO^+[^2\Sigma^+]$	$C[^3P_g]$	$^2\Sigma^-$, $^2\Pi$, $^4\Sigma^-$, $^4\Pi$
0	$CO[^1\Sigma^+]$	$C^+[^2P_u]$	$^2\Sigma^+$, $^2\Pi$

$R_{CO} \rightarrow \infty$:

Energy (cm^{-1})	Fragments		States for the linear molecule $[CCO]^+$
47821	$CC^+[^2\Pi_u]$	$O[^3P_g]$	$^2\Sigma^+$, $^2\Sigma^-$, $^2\Pi$, $^2\Delta$, $^4\Sigma^+$, $^4\Sigma^-$, $^4\Pi$, $^4\Delta$
40312	$CC^+[^4\Sigma_g^-]$	$O[^3P_g]$	$^2\Sigma^+$, $^2\Pi$, $^4\Sigma^+$, $^4\Pi$, $^6\Sigma^+$, $^6\Pi$

Table 2: Dominant configurations, energies and optimized linear geometries for the first electronic states of C_2O^+ calculated by CASSCF method and cc-pVTZ basis set (cf. text).

State / Configuration	R_{CC} (bohr)	R_{CO} (bohr)	Energy (hartree)
$^2\Pi$ $[...(1\pi^4)(7\sigma^2)(2\pi^1)]$	2.96 2.984[a]	2.11 2.132[a]	-150.320846
$^2\Delta$ $[...(1\pi^4)(7\sigma^1)(2\pi^2)]$	2.49	2.20	-150.240009
$^2\Sigma^+$ $[...(1\pi^4)(7\sigma^1)(2\pi^2)]$	2.47	2.23	-150.216771
$^2\Sigma^-$ $[...(1\pi^4)(7\sigma^1)(2\pi^2)]$	2.45	2.24	-150.211309
$^4\Sigma^-$ $[...(1\pi^4)(7\sigma^1)(2\pi^2)]$	2.57 2.551[b]	2.13 2.098[b]	-150.332491
$^4\Pi$ $[...(1\pi^3)(7\sigma^2)(2\pi^2)]$	2.64	2.47	-150.152082
$^4\Sigma^-$ $[...(1\pi^3)(7\sigma^1)(2\pi^3)]$	2.56	2.42	-150.113733

[a] : Maclagan and Sudkeaw [4] using MP2 / 6-31G**

[b] : Cao and Tian [5] using UHF / 6-31G*

Table 3: Equilibrium geometries (in bohr) and corresponding energies of the $^2\Pi$ and $^4\Sigma^-$ electronic states calculated with MRCI+Q and cc-pVnZ basis sets ($n = 2, 3, 4, 5$ (D, T, Q, 5)) [12].

Basis	$^2\Pi$			$^4\Sigma^-$			
	R_{CC}^{eq}	R_{CO}^{eq}	E (u.a.)	R_{CC}^{eq}	R_{CO}^{eq}	E (u.a.)	ΔE (cm^{-1})
cc-pVDZ	2.954	2.148	-150.505063	2.580	2.166	-150.493383	2569
cc-pVTZ	2.908	2.134	-150.621250	2.553	2.152	-150.610359	2393
cc-pVQZ	2.897	2.127	-150.657942	2.546	2.145	-150.647108	2378
cc-pV5Z	2.895	2.125	-150.669238	2.544	2.144	-150.658356	2388

Table 4: Polynomial expansion coefficients (in u.a.) of the PEFs, equilibrium geometries and equilibrium dipole moment of the $X^2\Pi$ state and of the $a^4\Sigma^-$ state.

Coefficient	$X^2\Pi$ (A";A')	$a^4\Sigma^-$
C_{000}	-150.669232	-150.658351
C_{200}	0.069364	0.236299
C_{110}	0.049029	0.095567
C_{020}	0.615323	0.572744
C_{002}	0.016401 ; 0.026488	0.053029
C_{300}	-0.094563	-0.247935
C_{210}	-0.049059	-0.094323
C_{120}	0.022997	0.024810
C_{030}	-0.837101	-0.790774
C_{102}	-0.000308 ; -0.019310	-0.022051
C_{012}	-0.028749 ; -0.033107	-0.054945
C_{400}	0.084199	0.160482
C_{310}	0.021903	0.065097
C_{220}	-0.003982	-0.021183
C_{130}	0.007584	0.009298
C_{040}	0.627665	0.588683
C_{202}	0.000258 ; 0.014961	-0.004466
C_{112}	0.032536 ; 0.043785	0.057973
C_{022}	0.005541 ; 0.005843	-0.002904
C_{004}	0.003978 ; 0.007067	0.006779
C_{500}	-0.042704	-0.093694
C_{600}	0.009368	0.040201
R_{CC}^{eq} (bohr)	2.8944	2.5433
R_{CO}^{eq} (bohr)	2.1235	2.1418
$\lvert\mu_e\rvert^a$ (D)	1.3665	2.7443

[a] the reference is taken at the center of mass.

Table 5: Spectroscopic constants (in cm^{-1}) of $X^2\Pi$ (A";A') and $a^4\Sigma^-$ electronic states obtained from PEFs given by equation 1.

	$X^2\Pi$		$a^4\Sigma^-$	
	MRCI+Q/cc-pV5Z	MP4SDQ/6-311G** [4]	MRCI+Q/cc-pV5Z	CISD/6-31G* [5]
ω_1	658.7	446	1171.4	1223.5
ω_2	262.3 ; 333.5	308	497.1	533.2
ω_3	2169.0	2285	2168.8	2320.1
x_{11}	-12.26		-2.41	
x_{12}	12.82 ; -78.54		14.19	
x_{22}	-1.57 ; 19.63		-3.08	
x_{13}	8.81		-16.14	
x_{23}	-6.42 ; -5.03		-10.04	
x_{33}	-18.62		-18.66	
x_{ll}	2.97; -18.50		3.79	
B_e	0.3487	0.3454^a	0.3996	

a HF value.

Table 6: Decomposition of stretching normal modes Q_1 and Q_3 on displacements of internal coordinates $\Delta R_{CC} = R_{CC} - R_{CC}^{eq}$ and $\Delta R_{CO} = R_{CO} - R_{CO}^{eq}$ from the analysis of PEFs given in Table 4.

State	Normal mode	ΔR_{CC}	ΔR_{CO}
$X^2\Pi$	Q_1	0.8599	0.5105
	Q_3	-0.0277	0.9996
$a^4\Sigma^-$	Q_1	0.8031	0.5959
	Q_3	-0.2310	0.9730

Table 7: Polynomial expansion coefficients of the spin-orbit function A of the $^2\Pi$ state. The reference is the equilibrium geometry of the $X^2\Pi$ electronic state.

Coefficient	(10^{-4} u.a.)				
C_{000}	-1.026284	C_{100}	0.568288	C_{010}	-0.478982
C_{200}	-0.500797	C_{110}	0.818086	C_{020}	-0.264850
C_{002}	0.213810	C_{300}	-0.021868	C_{210}	-0.141058
C_{120}	0.147772	C_{030}	0.002741	C_{102}	-0.207771
C_{012}	0.092577	C_{400}	0.240398	C_{310}	-0.653277
C_{220}	0.594445	C_{130}	-0.364503	C_{040}	0.060324
C_{202}	0.035374	C_{112}	0.075825	C_{022}	-0.117369
C_{004}	-0.015375	C_{500}	-0.029922	C_{600}	-0.079419

Table 8: Energies (in cm^{-1}) of the first rovibronic levels of the $X^2\Pi$ electronic state given with respect to the zero rovibrational energy at 1679.9 cm^{-1}.

$^2\Sigma_{1/2}\mu$		$^2\Sigma_{1/2}\kappa$		$^2\Pi_{1/2}$		$^2\Pi_{3/2}$	
v_1 v_2 v_3	Energy	v_1 v_2 v_3	Energy	v_1 v_2 v_3	Energy	v_1 v_2 v_3	Energy
0 1 0	249.5	0 1 0	393.6	0 0 0	0	0 0 0	44.5
0 3 0	764.0	1 1 0	1007.4	0 2 0 μ	514.2	0 2 0 μ	520.1
1 1 0	912.1	0 3 0	1080.5	1 0 0	645.3	1 0 0	680.5
0 5 0	1271.1	2 1 0	1607.2	0 2 0 κ	723.6	0 2 0 κ	726.8
1 3 0	1436.9	1 3 0	1680.5	0 4 0 μ	1022.6	0 4 0 μ	1027.3
2 1 0	1559.7	0 5 0	1779.0	1 2 0 μ	1181.0	1 2 0 μ	1190.2
0 7 0	1771.0			2 0 0	1273.5	2 0 0	1296.3
1 5 0*	1948.5			1 2 0 κ	1330.1	1 2 0* κ	1337.9
2 3 0*	2087.8			0 4 0 κ	1421.1	0 4 0 κ	1419.7
				0 6 0 μ	1525.9	0 6 0 μ	1531.0
				1 4 0 μ	1697.7	1 4 0 μ	1703.6
				2 2 0* μ	1825.4	2 2 0 μ	1843.4
				3 0 0	1893.1	2 2 0 κ	1896.6
				2 2 0* κ	1924.4	3 0 0	1936.7
				1 4 0* κ	2014.6	1 4 0* κ	2009.6
				0 8 0 μ	2025.8	0 8 0 μ	2036.2
				0 6 0 κ	2123.2	0 6 0* κ	2120.9
				0 0 1	2131.9	0 0 1	2177.2

$^2\Delta_{3/2}$		$^2\Delta_{5/2}$		$^2\Phi_{5/2}$		$^2\Phi_{7/2}$	
v_1 v_2 v_3	Energy	v_1 v_2 v_3	Energy	v_1 v_2 v_3	Energy	v_1 v_2 v_3	Energy
0 1 0	293.3	0 1 0	336.3	0 2 0	585.8	0 2 0	627.0
0 3 0 μ	788.3	0 3 0 μ	798.4	0 4 0 μ	1067.9	0 4 0 μ	1081.7
1 1 0	945.0	1 1 0	978.9	1 2 0	1244.8	1 2 0	1277.8
0 3 0 κ	1048.3	0 3 0 κ	1046.1	0 4 0 κ	1371.6	0 4 0 κ	1363.7
0 5 0 μ	1289.4	0 5 0 μ	1298.2	0 6 0 μ	1562.6	0 6 0 μ	1575.3
1 3 0 μ	1461.1	1 3 0 μ	1474.5	1 4 0 μ	1746.3	1 4 0 μ	1763.1
2 1 0	1580.1	2 1 0	1599.8	2 2 0	1887.1	2 2 0	1906.1
1 3 0 κ	1650.2	1 3 0* κ	1653.2	1 4 0 κ	1969.3	1 4 0 κ	1964.9
0 5 0 κ	1755.3	0 5 0* κ	1748.7	0 8 0* μ	2056.0	0 8 0* μ	2059.7
0 7 0 μ	1789.1	0 7 0 μ	1800.7	0 6 0 κ	2089.7	0 6 0* κ	2093.3
1 5 0* μ	1968.6	1 5 0* μ	1978.8				
2 3 0* μ	2112.7	2 3 0* μ	2132.9				

notations: μ, κ means that the level has a major weight on the A'', A' component respectively.
* tentative assignment.

Table 9: Energies of the first rovibrational levels of the $a^4\Sigma^-$ electronic state given with respect to the zero rovibrational energy at 2155.7 cm^{-1}.

$^4\Sigma^-$		$^4\Pi$		$^4\Delta$		$^4\Phi$	
v_1 v_2 v_3	Energy	v_1 v_2 v_3	Energy	v_1 v_2 v_3	Energy	v_1 v_2 v_3	Energy
0 0 0	0	0 1 0	494.1	0 2 0	989.6	0 3 0	1486.5
0 2 0	974.7	0 3 0	1459.0	0 4 0	1945.8	0 5 0	2434.9
1 0 0	1171.4	1 1 0	1676.8	1 2 0	2182.5	1 3 0	2688.6
0 4 0	1932.2	0 5 0	2409.4	0 6 0	2889.6	0 7 0	3372.3
0 0 1	2115.0	0 1 1	2599.4	0 2 1	3085.4	0 3 1	3572.9
1 2 0	2164.9	1 3 0	2656.8	1 4 0	3150.9	1 5 0	3646.9
2 0 0	2338.7	2 1 0	2855.8	2 2 0	3371.6	2 3 0	3886.8
0 6 0	2876.8	0 7 0	3348.3	0 8 0	3823.0	0 9 0	4300.4
0 2 1	3070.7	0 3 1	3545.9	0 4 1	4023.7	0 5 1	4503.8
1 4 0	3135.3	1 5 0*	3618.0	1 6 0*	4103.7	1 7 0*	4591.9
1 0 1	3271.0	1 1 1	3767.4	1 2 1	4264.2	1 3 1	4761.5
2 2 0	3350.1	2 3 0*	3849.3	2 4 0*	4350.6	2 5 0*	4853.5
3 0 0	3502.9	3 1 0	4032.0	3 2 0	4557.9		
0 8 0	3810.9	0 9 0	4277.6	0 10 0	4747.6		
0 4 1	4010.3	0 5 1	4478.9	0 6 1	4950.4		
1 6 0*	4089.4	1 7 0*	4565.1				
0 0 2	4197.1	0 1 2	4671.8				
1 2 1	4246.7	1 3 1	4729.9				
2 4 0*	4332.5	2 5 0*	4820.5				
2 0 1	4421.2	2 1 1	4930.2				
3 2 0*	4530.6						
4 0 0	4665.3						
0 10 0	4736.0						
0 6 1	4937.9						

* tentative assignment.

Table 10: First MRCI+Q / cc-pV5Z vertical transitions at the equilibrium geometry of the $X^2\Pi$ state for the doublet states and at the equilibrium geometry of the $a^4\Sigma^-$ for the quartet states.

Transition	$\Delta E\,(u.a.)$	$\Delta E\,(cm^{-1})$	$\Delta E\,(eV)$	$\lvert\vec{\mu}\rvert$ (Debye)
$X^2\Pi \rightarrow {}^2\Delta$	0.10563	23184	2.8745	0.475406
$X^2\Pi \rightarrow {}^2\Sigma^+$	0.13484	29593	3.6691	0.683866
$X^2\Pi \rightarrow {}^2\Sigma^-$	0.13870	30441	3.7743	0.638212
$a^4\Sigma^- \rightarrow {}^4\Pi$	0.19635	43093	5.3429	0.040129

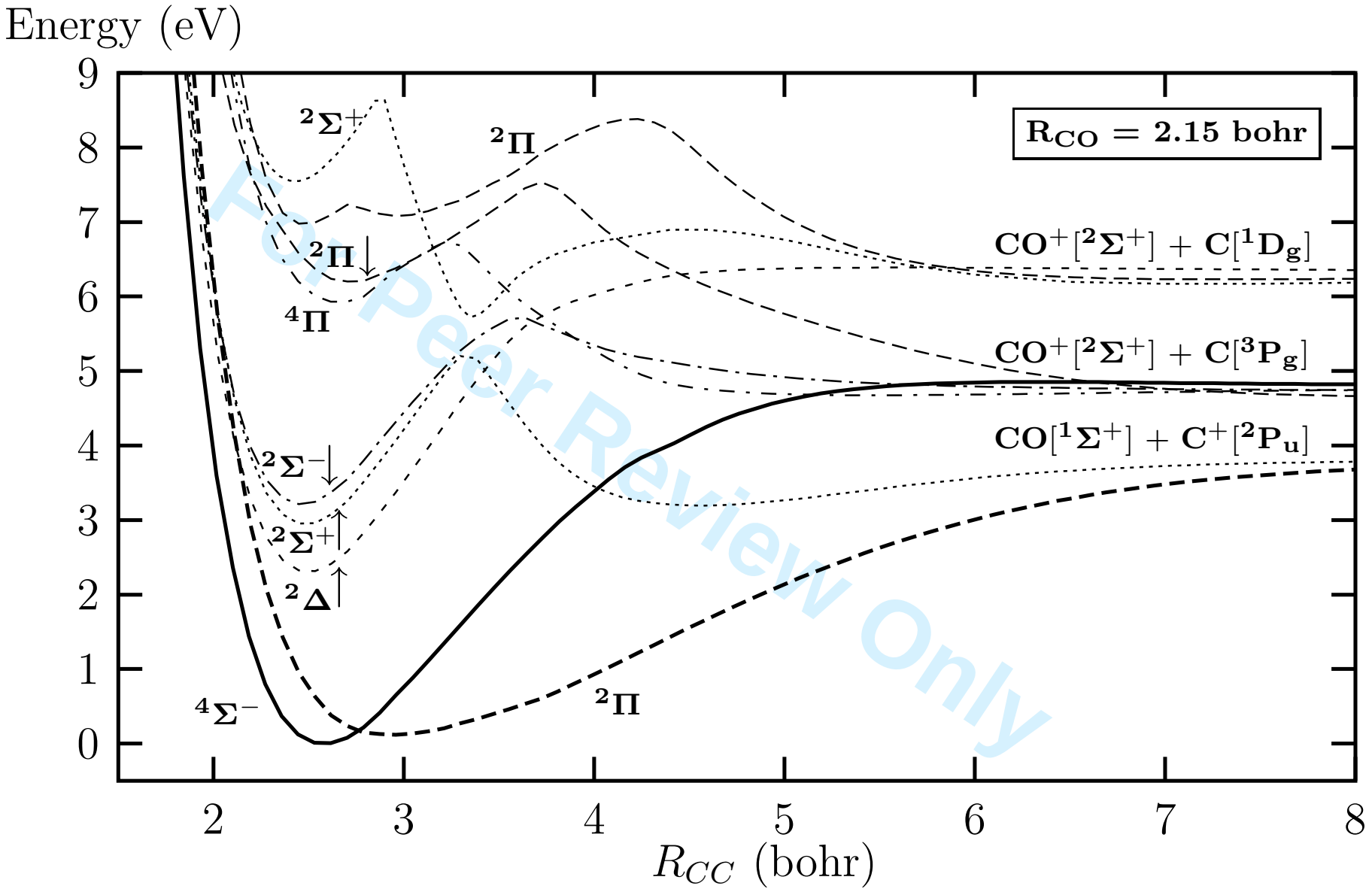

Figure 1:

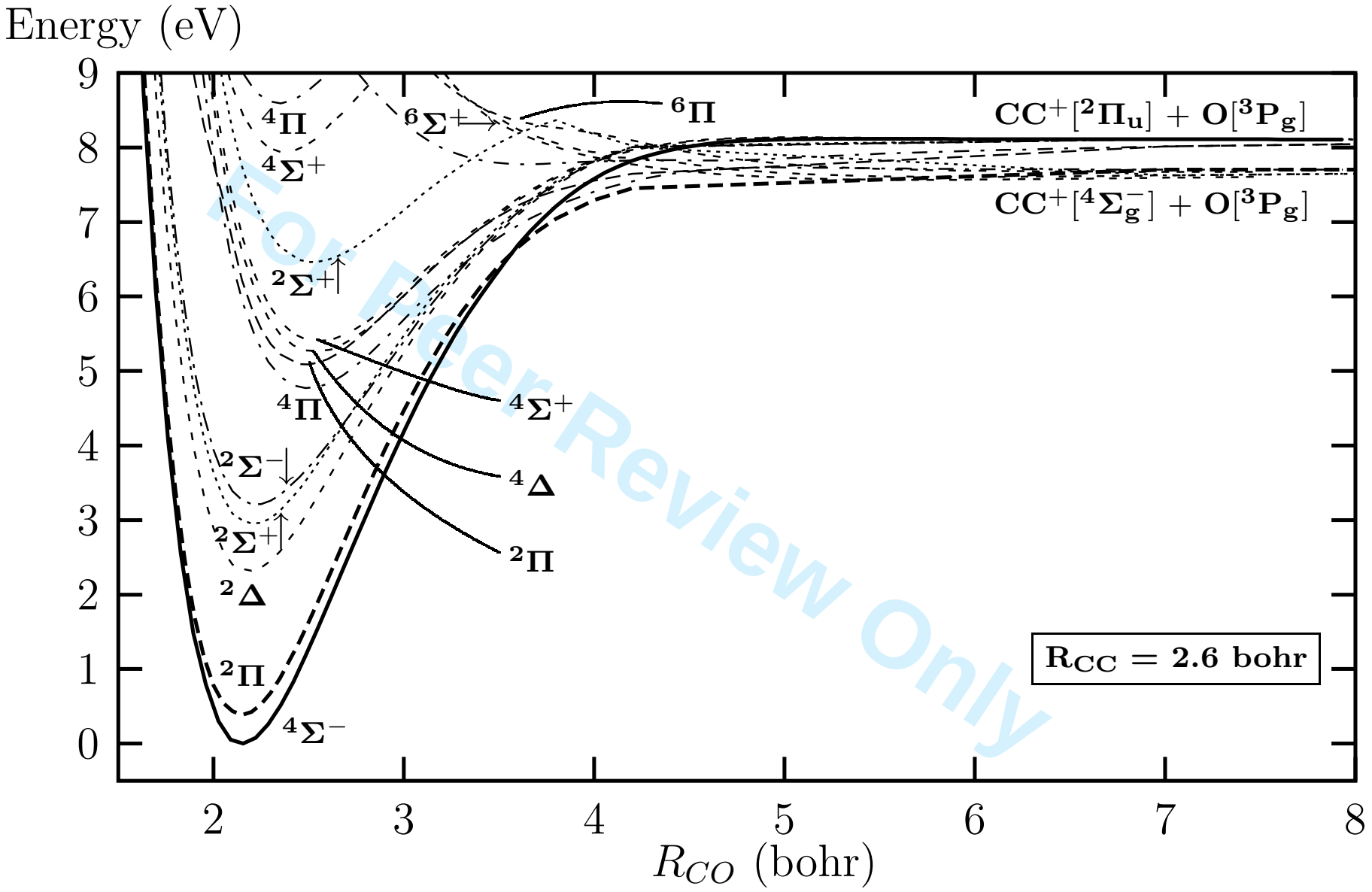

Figure 2:

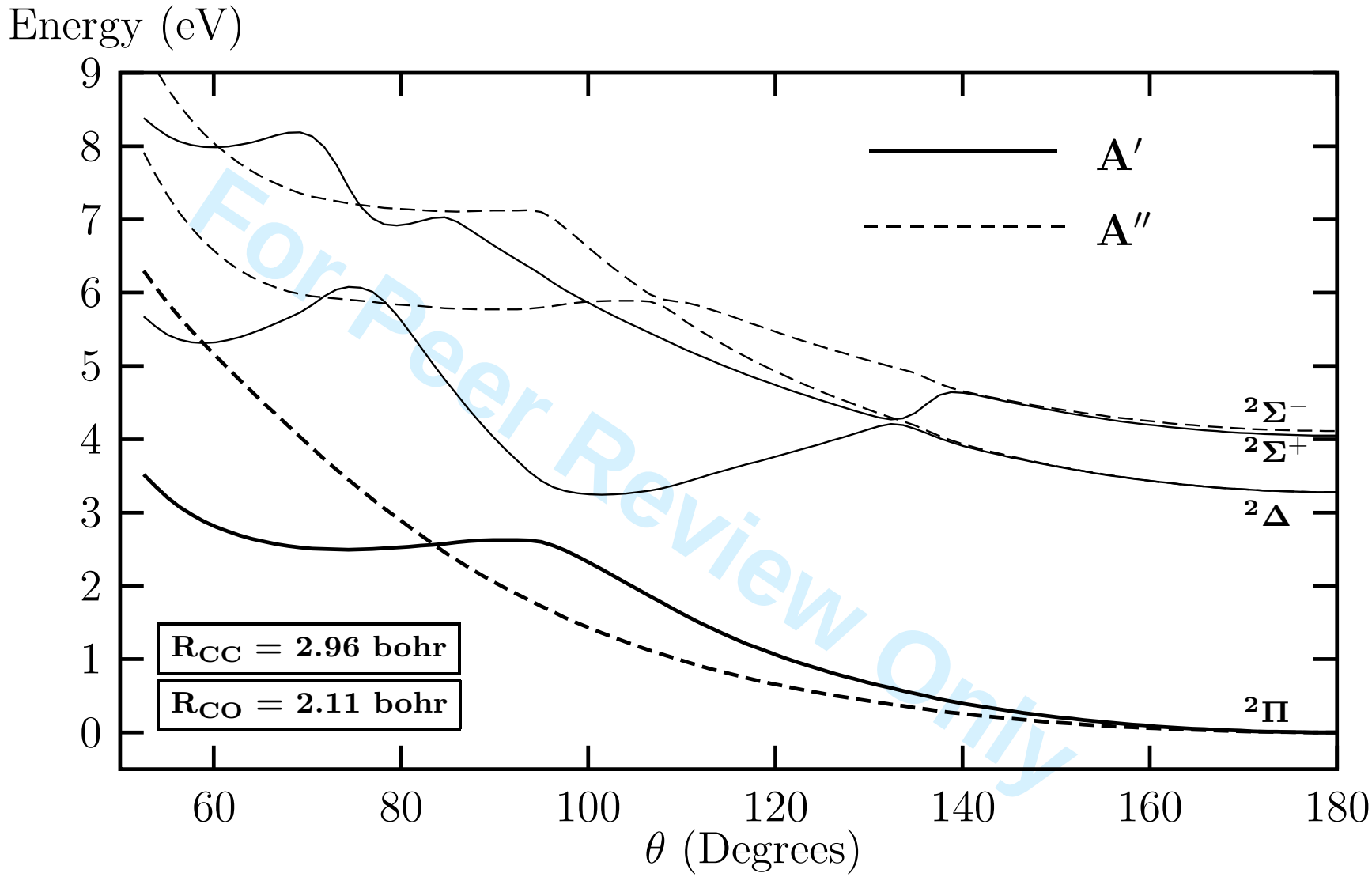

Figure 3:

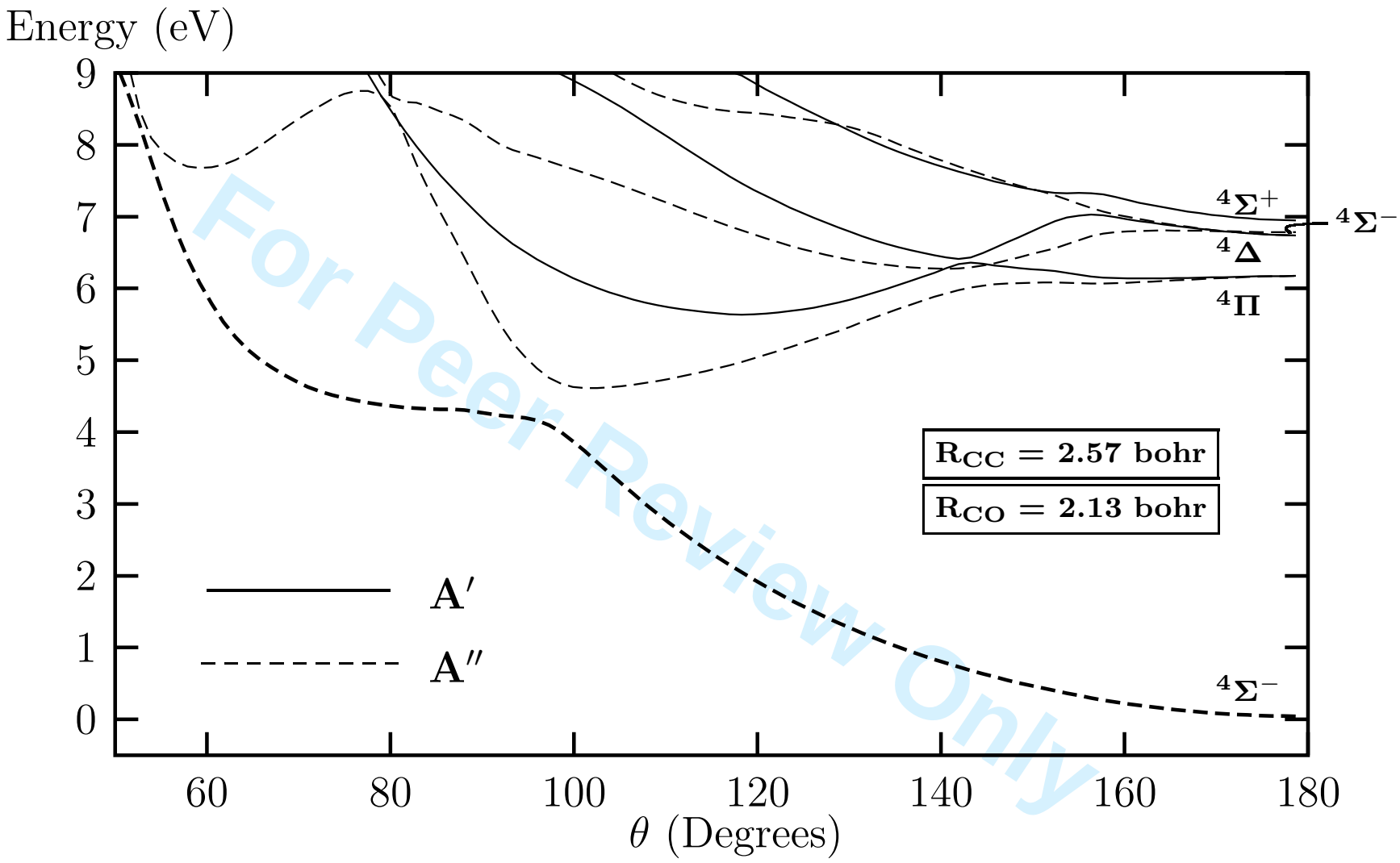

Figure 4:

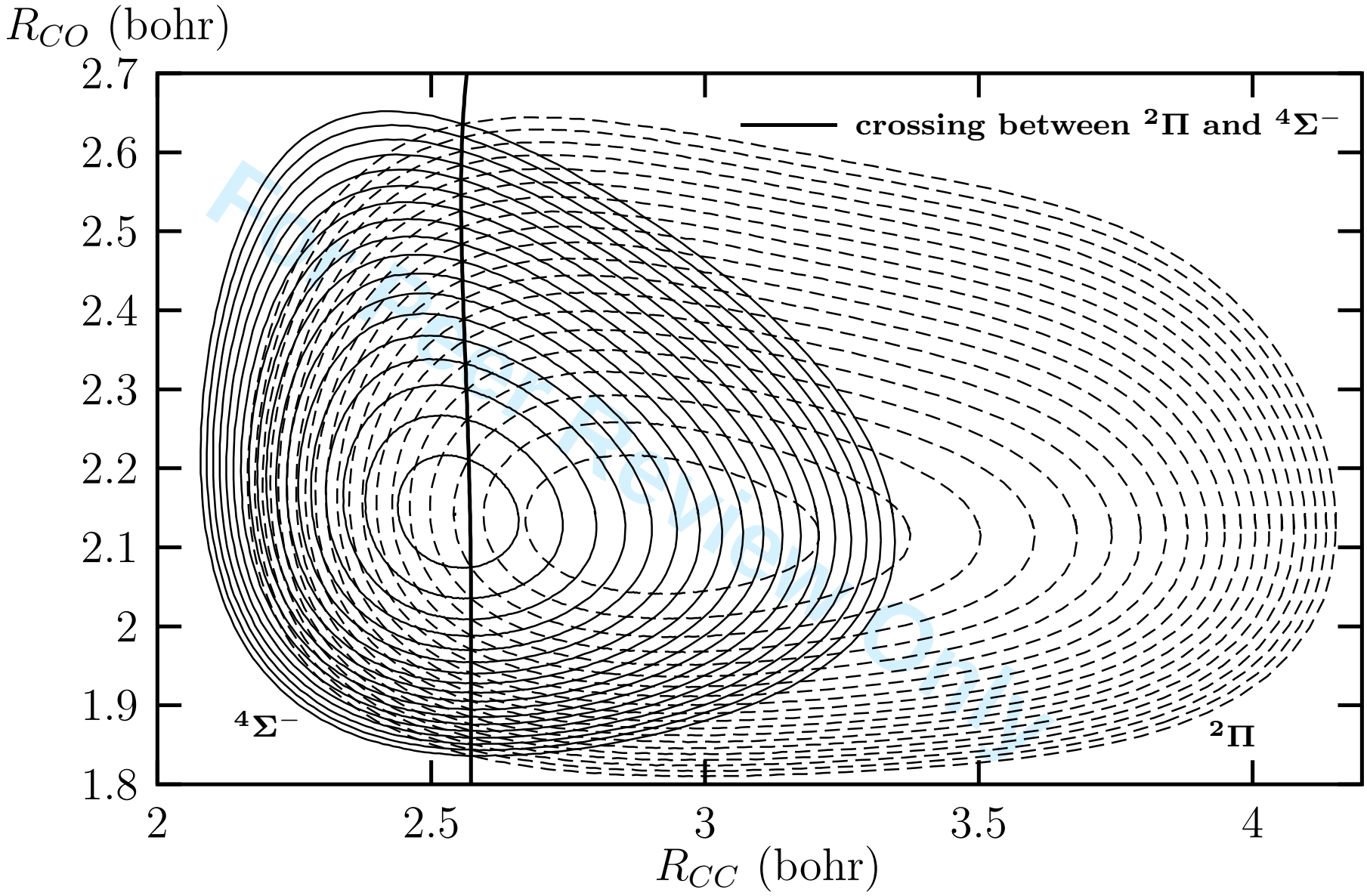

Figure 5:

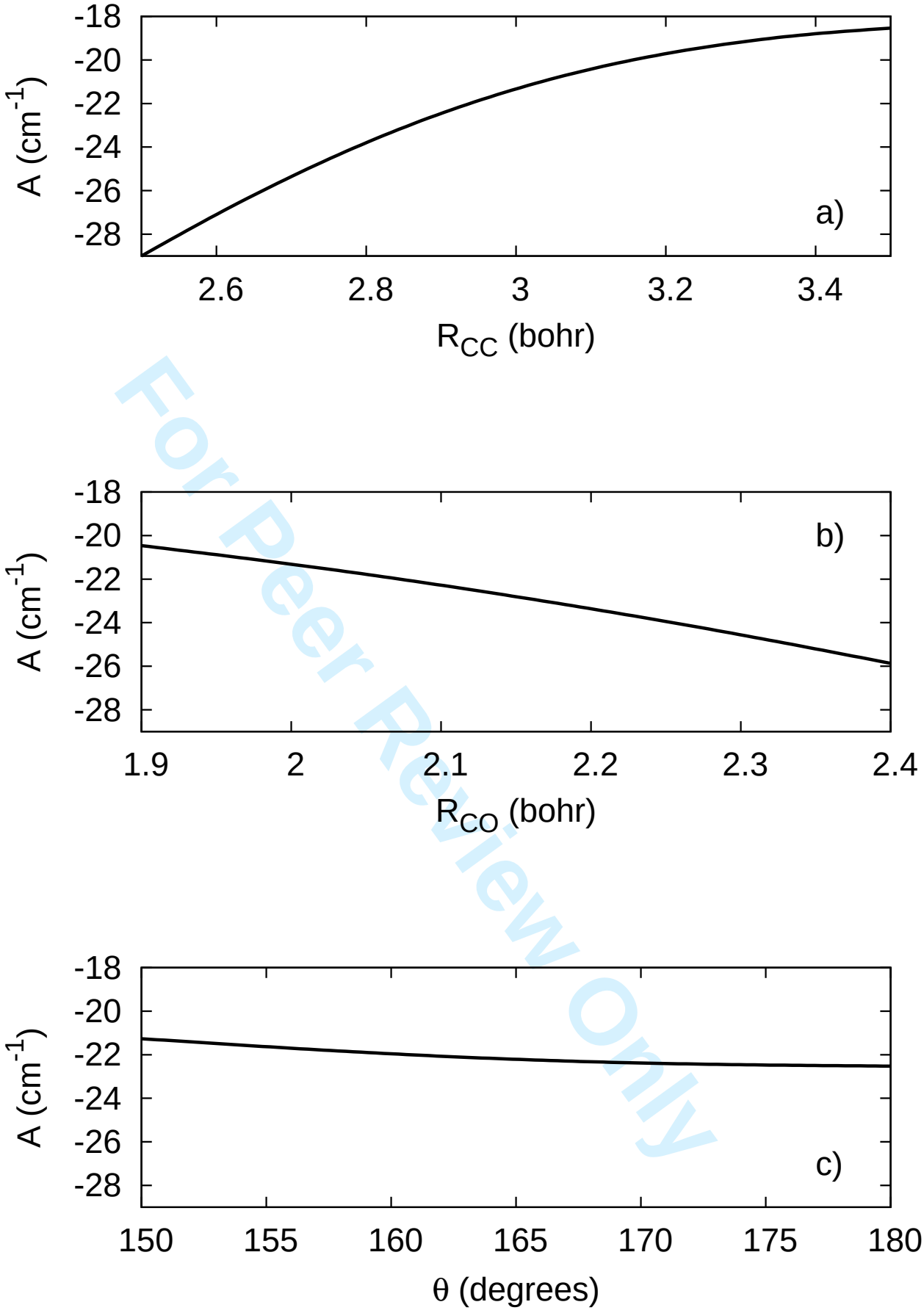

Figure 6:

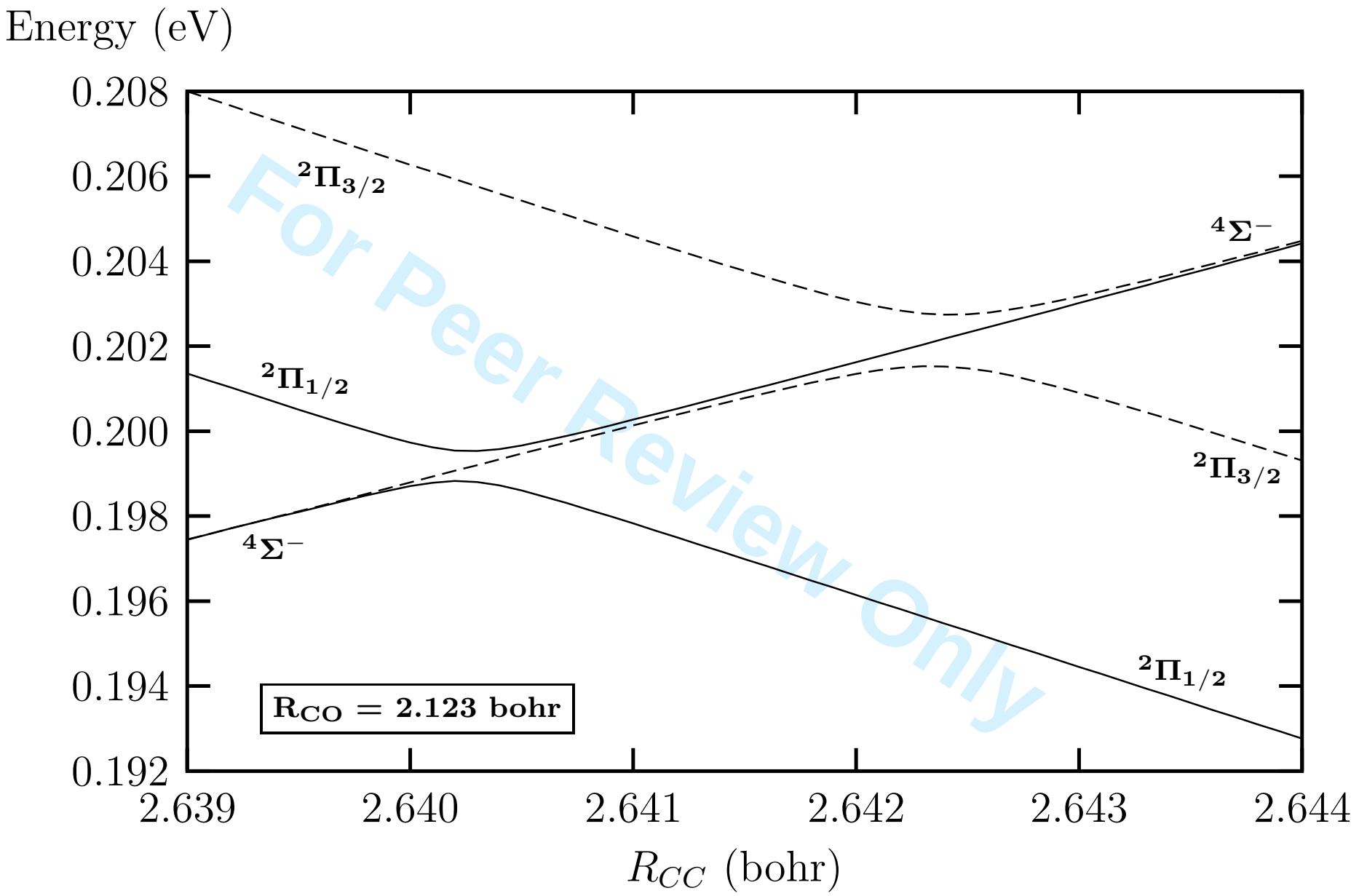

Figure 7: